

Fick Diffusion Coefficients of Liquid Mixtures Directly Obtained From Equilibrium Molecular Dynamics

Xin Liu,^{†,‡} Sondre K. Schnell,[‡] Jean-Marc Simon,[§] Dick Bedeaux,^{||} Signe Kjelstrup,^{||,‡} André Bardow,^{†,‡} and Thijs J. H. Vlugt^{*,‡}

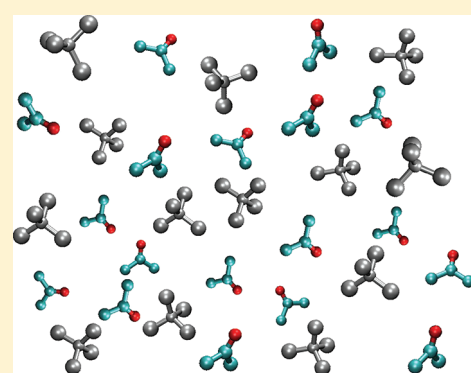
[†]Lehrstuhl für Technische Thermodynamik, RWTH Aachen University, Schinkelstrasse 8, 52062 Aachen, Germany

[‡]Process and Energy Laboratory, Delft University of Technology, Leeghwaterstraat 44, 2628 CA Delft, The Netherlands

[§]Laboratoire Interdisciplinaire Carnot de Bourgogne, UMR 5209 CNRS-Universite de Bourgogne, Dijon, France

^{||}Department of Chemistry, Norwegian University of Science and Technology, Trondheim, Norway

ABSTRACT: A methodology for computing Fick diffusivities directly from equilibrium molecular dynamics (MD) simulations is presented and validated for acetone–methanol and acetone–tetrachloromethane liquid mixtures. Fick diffusivities are obtained from Maxwell–Stefan (MS) diffusivities and the so-called thermodynamic factor. MS diffusivities describe the friction between different components, while the thermodynamic factor is the concentration derivative of the activity describing the deviation from ideal mixing behavior. It is important to note that all mutual diffusion experiments measure Fick diffusion coefficients, while molecular simulation provides MS diffusivities. The required thermodynamic factor to convert MS into Fick diffusivities and vice versa, however, is usually difficult to extract from both simulations and experiments leaving a gap between theory and application. Here, we employ our novel method to compute the thermodynamic factor from small-scale density fluctuations in equilibrium MD simulations [*Chem. Phys. Lett.* **2011**, *504*, 199–201]. Previously, this method was developed and validated for molecules with single interaction sites only. In this work, we applied this method to acetone–methanol and acetone–tetrachloromethane liquid mixtures and show that the method also works well in these more complex systems. This provides the missing step to extract Fick diffusion coefficients directly from equilibrium MD simulations. The computed Fick diffusivities of acetone–methanol and acetone–tetrachloromethane mixtures are in excellent agreement with experimental values. The suggested framework thus provides an efficient route to model diffusion in liquids on the basis of a consistent molecular picture.



1. INTRODUCTION

Understanding mass transport in liquids by mutual diffusion is an important topic for many applications in chemistry and chemical engineering.^{1,2} The reason for this is that diffusion is often the rate limiting step in chemical reactors and separators. To describe diffusive mass transport in liquid mixtures, generalized Fick's law and the Maxwell–Stefan theory are often used. In an n -component system, generalized Fick's law in a molar reference frame equals³

$$J_i = -c_t \sum_{j=1}^{n-1} D_{ij}^{\text{Fick}} \nabla x_j \quad (1)$$

in which J_i is the molar diffusion flux of component i , c_t is the total molar concentration, D_{ij}^{Fick} are Fick diffusivities, and x_j is the mole fraction of component j . The reference frame for the diffusion fluxes is the average molar velocity

$$\sum_{i=1}^n x_i u_i = u_{\text{reference}} \quad (2)$$

in which u_i is the average velocity of component i . From this it follows directly that $\sum_{i=1}^n J_i = 0$. Other reference frames, like the

barycentric, the mean volume, or the solvent frames of reference, are alternatively used depending on their convenience for experimental conditions. We refer to refs 4–6 for the transformation rules from one reference frame to the other. For binary mixtures, the resulting Fick diffusion coefficient is the same for all reference frames provided that one uses the gradient of the appropriate concentration in eq 1.⁴

Some problems arise when applying generalized Fick's law: (1) Fick diffusivities strongly depend on concentration, and in multicomponent systems, they can even be either positive or negative.^{1,7} (2) Multicomponent Fick diffusivities are unrelated to their binary counterparts which seriously hinders their prediction. (3) Generalized Fick's law is difficult to handle in practice due to the large number of concentration dependent coefficients; i.e., in an n -component system, $(n-1)^2$ diffusion coefficients are needed to describe transport. It is important to understand the concentration dependence of Fick diffusivities as

Received: August 30, 2011

Revised: September 27, 2011

Published: September 28, 2011

they directly relate to the measurable quantities, i.e., concentrations, and thus can be easily accessed in experiments. In fact, all mutual diffusion experiments measure Fick diffusion coefficients.

For describing multicomponent diffusion in liquids, the Maxwell–Stefan (MS) approach is often advocated.^{1,4,5} The key point of this approach is that the driving force for diffusion of component i (i.e., the chemical potential gradient $\nabla\mu_i$) is balanced by a friction force, resulting in the following equation

$$-\frac{1}{RT}\nabla\mu_i = \sum_{j=1, j \neq i}^n \frac{x_j(u_i - u_j)}{\mathfrak{D}_{ij}} \quad (3)$$

in which R and T are the gas constant and absolute temperature, respectively. The friction force between components i and j is proportional to the difference in average velocities of the components, $(u_i - u_j)$. The MS diffusivity \mathfrak{D}_{ij} is an inverse friction coefficient describing the magnitude of the friction between components i and j . The MS diffusivities are symmetric, $\mathfrak{D}_{ij} = \mathfrak{D}_{ji}$. Compared to generalized Fick's law, the MS theory requires only $n(n-1)/2$ diffusion coefficients for an n -component system, and they are all positive.¹ Often, MS diffusivities depend less strongly on concentration than Fick diffusivities.¹ It is difficult to obtain MS diffusivities directly from experiments as chemical potentials cannot be measured directly. Obtaining MS diffusivities from molecular dynamics (MD) simulations is possible but requires large amounts of CPU time.^{8–14}

As generalized Fick's law and the MS theory describe the same physical process, it is possible to relate the corresponding transport coefficients.^{1,4,5,8} The corresponding equation to relate the coefficients in eqs 1 and 3 is

$$[D_{ij}^{\text{Fick}}] = [B_{ij}]^{-1}[\Gamma_{ij}] \quad (4)$$

in which $[D_{ij}^{\text{Fick}}]$ is the $(n-1) \times (n-1)$ matrix of Fick diffusivities. The elements of the matrix $[B_{ij}]$ are given by^{3,4,8}

$$B_{ii} = \frac{x_i}{\mathfrak{D}_{in}} + \sum_{j=1, j \neq i}^n \frac{x_j}{\mathfrak{D}_{ij}} \text{ with } i = 1, \dots, (n-1) \quad (5)$$

$$B_{ij} = -x_i \left(\frac{1}{\mathfrak{D}_{ij}} - \frac{1}{\mathfrak{D}_{in}} \right) \text{ with } i, j = 1, \dots, (n-1) \quad (6)$$

The elements of the so-called matrix of thermodynamic factors $[\Gamma_{ij}]$ are defined by^{1,3,4,8}

$$\Gamma_{ij} = \delta_{ij} + x_i \left(\frac{\partial \ln \gamma_i}{\partial x_j} \right)_{T, p, \Sigma} \quad (7)$$

in which δ_{ij} is the Kronecker delta, and γ_i is the activity coefficient of component i . The symbol Σ is used to indicate that the differentiation is carried out while keeping constant the mole fractions of all other species except the n -th, so that the mole fractions always sum to unity. In binary mixtures, transport diffusion is described by a single MS and a single Fick diffusion coefficient, and they are related by

$$D^{\text{Fick}} = \Gamma \times \mathfrak{D}_{12} \quad (8)$$

in which the thermodynamic factor Γ is given by⁴

$$\Gamma = 1 + x_1 \left(\frac{\partial \ln \gamma_1}{\partial x_1} \right)_{T, p, \Sigma} \quad (9)$$

For an ideal binary gas mixture, $\Gamma \equiv 1$. Equation 8 nicely visualizes the gap between experimental and molecular simulation approaches to mutual diffusion: in experiments, Fick diffusion coefficients are measured and molecular simulation usually provides MS diffusivities.^{9,15–18} The two worlds could be related via the thermodynamic factor Γ , but this is known only with large uncertainties.^{19,20}

In this work, we introduce a consistent and efficient framework for the determination of Fick diffusivities in liquid mixtures directly from equilibrium MD simulations by calculating both the thermodynamic factor Γ and the MS diffusivity \mathfrak{D}_{12} . Up to now, approaches to compute Fick diffusivities from molecular simulation suffer from inconsistencies or other problems: (1) Direct calculation of Fick diffusivities using nonequilibrium MD (NEMD) requires significant efforts, and very high concentration gradients are needed.^{21–23} This approach is usually not accurate and quite impractical as the concentration dependence of Fick diffusivities is not easily captured. (2) Combining MS diffusivities obtained from equilibrium MD simulations with experimentally obtained equations of state or models for the excess Gibbs energy is inconsistent as experiments and molecular models in principle provide different values for the thermodynamic factor.^{18,24,25} (3) Presently used molecular simulation techniques to determine the thermodynamic factor of liquid mixtures are inefficient.^{17,26} Recently, we developed an efficient method to obtain the thermodynamic factor directly from equilibrium MD simulations.^{26,27} This method is based on sampling concentration fluctuations inside small subvolumes inside the simulation box and correcting for finite-size effects. We already validated this method for simple systems with only a single interaction site per molecule, i.e., mixtures in which the components interact using Weeks–Chandler–Andersen (WCA) or Lennard–Jones (LJ) interaction potentials. In this work, we implemented the method for the more complex mixtures of acetone–methanol and acetone–tetrachloromethane (CCl_4). Thereby, we can efficiently compute the thermodynamic factor Γ such that, in combination with computed MS diffusivities, we are able to compute Fick diffusion coefficients directly from equilibrium MD. Our MD results for Γ , \mathfrak{D}_{12} , and D^{Fick} also agree very well quantitatively with the experiments suggesting that the tools for computing multicomponent Fick diffusivities from MD simulations are now available.

This paper is organized as follows. In section 2, we explain how to obtain the MS diffusivities and thermodynamic factors from equilibrium MD simulations, and we also provide a brief review of predictive models for diffusion coefficients. The details concerning the MD simulations are addressed in section 3. In section 4, we validate the methodology for computing Fick and MS diffusivities for the binary mixtures acetone–methanol and acetone– CCl_4 . Our conclusions are summarized in section 5.

2. DIFFUSION COEFFICIENTS AND THERMODYNAMIC FACTOR

2.1. Obtaining Diffusion Coefficients from MD Simulations.

In equilibrium MD simulations, representative trajectories of a liquid mixture consisting of interacting molecules can be obtained.^{28–30} From the trajectory of the molecules, transport properties can be computed.²⁸ The self-diffusivity describes the motion of individual molecules. The Einstein equation connects the self-diffusivity $D_{i,\text{self}}$ of component i to the average molecular displacements of molecules of type i ²⁸

$$D_{i,\text{self}} = \frac{1}{6N_i} \lim_{m \rightarrow \infty} \frac{1}{m \cdot \Delta t} \left\langle \left(\sum_{l=1}^{N_i} (r_{i,l}(t + m \cdot \Delta t) - r_{i,l}(t))^2 \right) \right\rangle \quad (10)$$

Here, N_i is the total number of molecules of component i , m is the number of time steps in the MD simulation, Δt is the time step used in the MD simulation, and $r_{l,i}(t)$ is the position of the l th molecule of component i at time t . In our computations, the mean squared displacement is updated with different frequencies according to the order- n algorithm described in refs 28 and 31.

MS diffusivities \mathfrak{D}_{ij} can also be obtained from the motion of the molecules.²⁸ First, the Onsager coefficients Λ_{ij} are calculated:⁸

$$\Lambda_{ij} = \frac{1}{6m} \lim_{m \rightarrow \infty} \frac{1}{N} \frac{1}{m \cdot \Delta t} \left\langle \left(\sum_{l=1}^{N_i} (r_{l,i}(t + m \cdot \Delta t) - r_{l,i}(t)) \right) \times \left(\sum_{k=1}^{N_j} (r_{k,j}(t + m \cdot \Delta t) - r_{k,j}(t)) \right) \right\rangle \quad (11)$$

These coefficients are constrained by $\sum_{i=1}^n M_i \Lambda_{ij} = 0$ in which M_i is the molar mass of component i .⁸ Furthermore, $\Lambda_{ij} = \Lambda_{ji}$. An alternative but equivalent form of eq 11 is

$$\Lambda_{ij} = \frac{1}{3N} \int_0^\infty dt \left\langle \sum_{l=1}^{N_i} v_{l,i}(0) \cdot \sum_{k=1}^{N_j} v_{k,j}(t) \right\rangle \quad (12)$$

In eqs 11 and 12, N is the total number of molecules and i, j are the molecule types. $v_{l,i}(0)$ and $v_{k,j}(t)$ are the velocities of the l th molecule of component i at time 0 and the velocities of the k th molecule of component j at time t , respectively. Using the computed values for Λ_{ij} and the mixture composition, MS diffusivities can easily be computed. In binary mixtures, we obtain the following expression for MS diffusivities in terms of the Onsager coefficients:

$$\mathfrak{D}_{12} = \left[\frac{x_2}{x_1} \Lambda_{11} + \frac{x_1}{x_2} \Lambda_{22} - 2\Lambda_{12} \right] \quad (13)$$

The expressions relating the Onsager coefficients Λ_{ij} to the MS diffusivities in ternary and quaternary mixtures are algebraically more complex and can be found in refs 8 and 11

Computing binary Fick diffusion coefficients directly from equilibrium MD simulations requires the use of eq 8 and separate calculations of the MS diffusivity \mathfrak{D}_{12} and the thermodynamic factor Γ .

2.2. Predictive Models for Diffusion. To obtain a better understanding of the concentration dependence of MS diffusivities, it is instructive to study the different contributions of the correlation function in eq 12, i.e., velocity auto- and cross-correlations. These contributions are defined as follows. Considering the Green–Kubo form of the Onsager coefficients (eq 12), we can express Λ_{ii} as

$$\begin{aligned} \Lambda_{ii} &= \frac{1}{3N} \int_0^\infty dt \left\langle \sum_{l=1}^{N_i} v_{l,i}(0) \cdot \sum_{g=1}^{N_i} v_{g,i}(t) \right\rangle \\ &= \frac{1}{3N} \int_0^\infty dt \left\langle \sum_{l=1}^{N_i} v_{l,i}(0) \cdot v_{l,i}(t) \right\rangle \\ &\quad + \frac{1}{3N} \int_0^\infty dt \left\langle \sum_{l=1}^{N_i} \sum_{g=1, g \neq l}^{N_i} v_{l,i}(0) \cdot v_{g,i}(t) \right\rangle \\ &\approx x_i C_{ii} + x_i^2 N C_{ii}^* \\ &= x_i D_{i,\text{self}} + x_i^2 N C_{ii}^* \end{aligned} \quad (14)$$

in which C_{ii} and C_{ii}^* account for self- and cross-correlations of the velocities of molecules of component i , respectively. Here, we

assumed that $N_i^2 - N_i \approx N_i^2$. For Λ_{ij} with $i \neq j$, i.e., the correlations between unlike molecules, we can write¹⁰

$$\begin{aligned} \Lambda_{ij} &= \frac{1}{3N} \int_0^\infty dt \left\langle \sum_{l=1}^{N_i} v_{l,i}(0) \cdot \sum_{k=1}^{N_j} v_{k,j}(t) \right\rangle \\ &\approx \frac{N_i N_j}{3N} \int_0^\infty dt \langle v_{1,i}(0) \cdot v_{1,j}(t) \rangle \\ &= N x_i x_j C_{ij} \end{aligned} \quad (15)$$

For a binary system, combining eqs 10 and 15 leads to

$$\begin{aligned} \mathfrak{D}_{12} &= x_2 C_{11} + x_1 C_{22} + x_1 x_2 N (C_{11}^* + C_{22}^* - 2C_{12}) \\ &= x_2 D_{1,\text{self}} + x_1 D_{2,\text{self}} + x_1 x_2 N (C_{11}^* + C_{22}^* - 2C_{12}) \end{aligned} \quad (16)$$

In so-called ideal diffusing mixtures, the terms C_{ii}^* and C_{ij} are small compared to terms of the type C_{ii} resulting in the well-known binary Darken equation:^{11,32}

$$\mathfrak{D}_{ij} = x_j D_{i,\text{self}} + x_i D_{j,\text{self}} \quad (17)$$

A natural extension of eq 17 to multicomponent systems was presented in ref 11. It is important to note that the application of the Darken equation relies on the availability of self-diffusivities in the mixture. To parametrize the Darken equation, we recently proposed the following model to predict self-diffusivities in multicomponent systems from data at infinite dilution:¹¹

$$\frac{1}{D_{i,\text{self}}} = \sum_{j=1}^n \frac{x_j}{D_{i,\text{self}}^{x_j \rightarrow 1}} \quad (18)$$

We have shown that eq 18 works well for WCA fluids and the ternary mixture n-hexane/toluene/cyclohexane.¹¹

2.3. Obtaining the Thermodynamic Factor from MD Simulations. The elements of the matrix $[\Gamma_{ij}]$ can be expressed as average concentration fluctuations in the grand-canonical ensemble as derived by Kirkwood and Buff^{33,34} in 1951. The natural method for obtaining these averages are grand-canonical Monte Carlo (GCMC) simulations. However, GCMC simulations of liquid mixtures at room temperature are very challenging as the insertion and deletion of molecules is very inefficient for dense liquids.²⁸ There is some recent improvement in this area,^{35,36} but these simulations remain quite inefficient. Kirkwood and Buff showed that the fluctuations in the grand-canonical ensemble can be related to the integrals of radial distribution functions over volume,^{33,34} resulting in the following expression for the so-called Kirkwood–Buff (KB) coefficients:

$$G_{ij} = V \frac{\langle N_i N_j \rangle - \langle N_i \rangle \langle N_j \rangle}{\langle N_i \rangle \langle N_j \rangle} - \frac{\delta_{ij}}{c_i} \quad (19)$$

$$= 4\pi \int_0^\infty [g_{ij}(r) - 1] r^2 dr \quad (20)$$

In these equations, V is the volume and c_i is the number density of component i defined by $\langle N_i \rangle / V$. The brackets $\langle \dots \rangle$ denote an ensemble average in the grand-canonical ensemble. $g_{ij}(r)$ is the radial distribution function for molecules of type i and j in the grand-canonical ensemble, and it is natural to define the distance r between two molecules as the distance between their centers of mass. As the choice of ensemble is irrelevant for large systems, in practice $g_{ij}(r)$ is computed in the NpT or NVT ensemble. In binary mixtures, the thermodynamic factor Γ is related to the KB

Table 1. Force Field and Geometrical Parameters for Acetone, Methanol, and CCl₄^a

		Force Field Parameters		
site		$\sigma/\text{\AA}$	$(\epsilon/k_B)/\text{K}$	q/e
CH ₃	(acetone)	3.910	81.0866	0.0620
C	(acetone)	3.750	52.9463	0.3000
O	(acetone)	2.960	105.8997	−0.4240
C	(CCl ₄)	3.410	50.3972	−0.1616
Cl	(CCl ₄)	3.450	143.6321	0.0404
O	(methanol)	3.070	85.6753	−0.7000
H	(methanol)			0.4350
CH ₃	(methanol)	3.775	104.3223	0.2650

Geometrical Parameters			
bond length/ \AA		bond angle/deg	
C—Cl	1.766	CH ₃ —C—CH ₃	116.30
C=O	1.220	CH ₃ —C=O	121.86
CH ₃ —C	1.507	Cl—C—Cl	109.47
O—H	0.945	CH ₃ —O—H	108.50
CH ₃ —O	1.430		

^a Parameters for acetone and CCl₄ were taken from ref 40. Parameters for methanol were taken from ref 39.

coefficients G_{ij} by^{27,33}

$$\Gamma = 1 - x_i \frac{c_j(G_{ii} + G_{jj} - 2G_{ij})}{1 + c_j x_i (G_{ii} + G_{jj} - 2G_{ij})} \quad (21)$$

For ternary systems, the values of the terms Γ_{ij} (eq 7) follow in a similar way from the values of the KB coefficients G_{ij} .³⁷

It is important to consider the convergence of the integrals in eq 20. For infinitely large systems, $g_{ij}(r) \rightarrow 1$ for $r \rightarrow \infty$. For finite systems with periodic boundary conditions, $g_{ij}(r)$ does not converge to 1 for $r \rightarrow \infty$, and therefore, in practice corrections have to be taken into account.^{26,27,38} This seriously hinders the direct estimation of Kirkwood–Buff (KB) coefficients from simulations.

Recently, we found that the average particle fluctuations in eq 19 can also be calculated by considering a large system in which smaller subvolumes are embedded. The subvolumes can exchange particles and energy with the simulation box, and therefore, a subvolume can be considered as a system in the grand-canonical ensemble. However, corrections should be taken due to the finite size effect originating from the boundaries of the subvolumes:^{26,27}

$$G_{ij}(L) = G_{ij}^{\infty} + \frac{(\text{constant})}{L} \quad (22)$$

In this equation, L is the (linear) size of the subsystem in one dimension. The KB coefficient in the thermodynamic limit (G_{ij}^{∞}) can thus be obtained by simple extrapolation to $L \rightarrow \infty$. This approach was previously validated for molecules with a single interaction site only, e.g., systems in which the particle interact using a WCA or Lennard-Jones (LJ) potential. In practice, the size of the simulation box needs to be at least 10 times the size of a typical molecule in the system.²⁶ For more details concerning this method, we refer the reader to refs 26 and 27.

Table 2. Densities and Self-Diffusivities of Pure Acetone, Methanol, and CCl₄ at 298 K, 1 atm

component	$\rho / (\text{g mL}^{-1})$		$D_{i,\text{self}} / (10^{-9} \text{ m}^2 \text{ s}^{-1})$	
	this work (MD)	experiment	this work (MD)	experiment
acetone	0.76	0.78, ^{a,b} 0.79 ^c	4.2	4.8, ^d 4.4 ^e
methanol	0.75	0.79 ^{a,b}	2.5	2.3, ^f 2.2 ^g
CCl ₄	1.54	1.58 ^c	1.8	1.5 ^d

^a Experiments by Campbell et al., ref 45. ^b Experiments by Noda et al., ref 46. ^c Experiments reported in ref 47. ^d Experiments by Hardt et al., ref 41. ^e Experiments by Toryanik et al., ref 42. ^f Experiments by Kamei et al., ref 43. ^g Experiments by Derlacki et al., ref 44.

3. MOLECULAR DYNAMICS SIMULATIONS

The binary systems acetone–methanol and acetone–CCl₄ were studied. The OPLS force field was used for acetone and methanol,^{39,40} and a nonpolarizable five-site model was used for CCl₄.⁴⁰ All components are treated as rigid bodies. The LJ potentials describe the intermolecular nonbonded interactions which are truncated and shifted at 10 \AA . The Lorentz–Berthelot mixing rules are applied to obtain the LJ parameters for the interaction of unlike atoms.²⁹ Electrostatic interactions are handled by Ewald summation using a relative precision of 10^{-5} . The force field parameters as well as the parameters defining the geometries of the molecules are listed in Table 1. Three dimensional periodic boundary conditions consistent with a cubic box were applied to obtain properties corresponding to bulk systems. The MD simulations were carried out at a temperature of 298 K and a pressure of 1 atm. All binary systems were first equilibrated in an NpT ensemble with a Nosé–Hoover thermostat and barostat using the time constants of 0.1 and 1 ps, respectively. The equations of motion were integrated using the leapfrog Verlet algorithm with a time step of 1 fs. The self-diffusion and MS diffusion coefficients are obtained from equilibrium MD simulations in the NVT ensemble using the Nosé–Hoover thermostat at a density corresponding to a pressure of 1 atm.²⁸ The box sizes were typically around $(28 \text{ \AA})^3$ resulting in a total number of molecules of the order of 300. The simulations for extracting diffusion coefficients were run for at least 100 ns to obtain MS diffusivities with an accuracy of around 5% and self-diffusivities with an accuracy of 2%. KB coefficients required for the calculation of thermodynamic factors were obtained from MD simulations in the NpT ensemble. Temperature and pressure were controlled using the Nosé–Hoover thermostat and barostat, respectively. In these simulations, the box size needs to be larger, see also section 2.3. The box size was typically fluctuating around $(80 \text{ \AA})^3$. The maximum number of molecules used in these simulations was 8000. Simulation runs of at least 20 ns were needed to obtain accurate values (errors smaller than 5%) of the thermodynamic correction factor. On a typical workstation, this takes around 2 weeks of CPU time.

4. RESULTS AND DISCUSSION

4.1. Model Validation for Pure Component Systems. In Table 2, we compare the computed densities and self-diffusivities of the pure components to the experimental results. For all three components, MD simulations underestimate the densities of the pure components by a maximal deviation of 3%. This directly

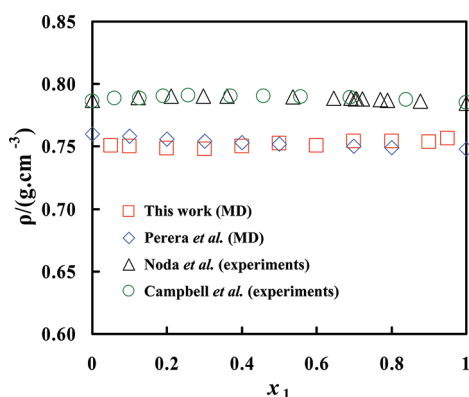


Figure 1. Densities of acetone (1)–methanol (2) mixtures at 298 K, 1 atm. Squares are the computed densities by this work using MD simulations. Diamonds are the computed densities by Perera et al. using MD simulations.³⁸ Circles are the experimental densities measured by Campbell et al.⁴⁵ Triangles are the experimental densities measured by Noda et al.⁴⁶

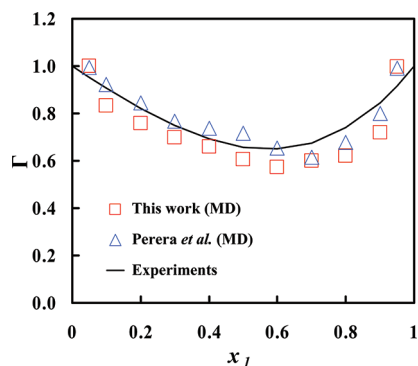


Figure 2. Thermodynamic factor Γ (eq 9) in acetone (1)–methanol (2) mixtures at 298 K, 1 atm. Squares are the computed Γ by this work using MD simulations (error bars are equal to the symbol size). Triangles are the computed Γ by Perera et al. using MD simulations.³⁸ The solid line represents Γ calculated from experimental VLE data taken from ref 50.

results in a small overestimation of self-diffusivities in most cases, i.e., for pure methanol and pure CCl_4 . The computed self-diffusivities of pure acetone, pure methanol, and pure CCl_4 are 4.2 , 2.5 , and $1.8 \times 10^{-9} \text{ m}^2 \text{ s}^{-1}$, respectively. Several values for the experimental self-diffusivity of pure acetone are available ranging from 4.4 to $4.8 \times 10^{-9} \text{ m}^2 \text{ s}^{-1}$.^{41,42} For pure methanol, experimental self-diffusivities reported in literature range from 2.2 to $2.3 \times 10^{-9} \text{ m}^2 \text{ s}^{-1}$.^{43,44} The reported experimental self-diffusivity of pure CCl_4 is $1.5 \times 10^{-9} \text{ m}^2 \text{ s}^{-1}$.^{41,43} The maximal deviation of the computed self-diffusivities from experiments is thus 20%. We feel that this level of deviation between experiments and simulations is acceptable in our study. Noteworthy, the force fields used have not been fitted to transport properties. Thus, the presented results are predictive.

4.2. Diffusion in Acetone–Methanol. Figure 1 compares the computed densities of acetone–methanol mixtures to the experimental data at 298 K, 1 atm. The computed mixture densities from this work are consistent with the data obtained by Perera et al. using MD simulations.³⁸ However, the results obtained from simulations are systematically somewhat lower than the

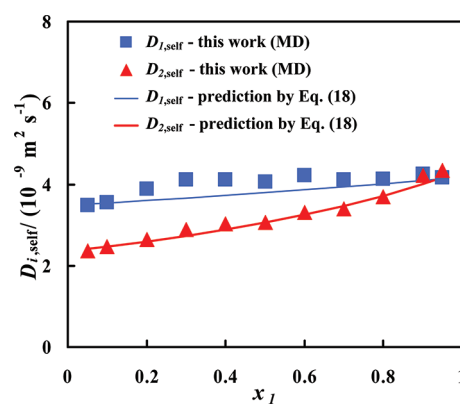


Figure 3. Self-diffusivities in acetone (1)–methanol (2) mixtures at 298 K, 1 atm. Filled symbols are the computed self-diffusivities by this work using MD simulations. Solid lines are the predictions using eq 18.

experimental densities.^{45,46} In acetone–methanol mixtures, both experiments and simulations show that densities are not sensitive to the composition.

Figure 2 shows how the thermodynamic factor Γ varies with concentration. We observe that both the computed Γ in this work and the computations by Perera et al.³⁸ agree very well with experiments. Note that the data of Perera et al.³⁸ seems to have an inflection point around equimolar composition, which appears to be unphysical and due to limited accuracy in their simulations. The dependence of Γ on concentration is accurately described by our simulations. It is important to note that there are obvious differences between our simulations and those of Perera et al. Perera et al.³⁸ obtained the KB coefficients by directly integrating the radial distribution functions over the volume (eq 20), while we used the novel fluctuation method described in section 2.3. The agreement between the two methods clearly shows that macroscopic properties can be extrapolated from microscopic systems by applying finite-size corrections. The proposed fluctuation method is therefore not only valid in simple systems, e.g., WCA systems and homogeneous LJ systems. The presented results demonstrate that the fluctuation method also works well for complicated molecular systems in which electrostatic interactions play an important role.

Figure 3 shows self-diffusivities in acetone–methanol mixtures as a function of the composition. We are not aware of any experimental results for the self-diffusivities in acetone–methanol mixtures. To describe the dependence of self-diffusivities on concentration, eq 18 is used which requires the self-diffusivities at infinite dilution. Figure 3 clearly shows that eq 18 correctly captures the behavior of the self-diffusivities; i.e., as the concentration of acetone is increasing, the self-diffusivities of both components increase, and the self-diffusivities of methanol show a stronger dependence on concentration.

Figure 4 compares the computed MS diffusivities using MD simulations (eq 13) to the predictions using the Darken equation (eq 17). The self-diffusivities needed in the Darken equation are parametrized with both MD data and predictions using eq 18. As eq 18 accurately describes the dependence of self-diffusivities on concentration, the differences between both parametrizations are small. There is, however, a significant difference between the computed MS diffusivities and the predicted MS diffusivities using the Darken equation. In MD simulations, MS diffusivities

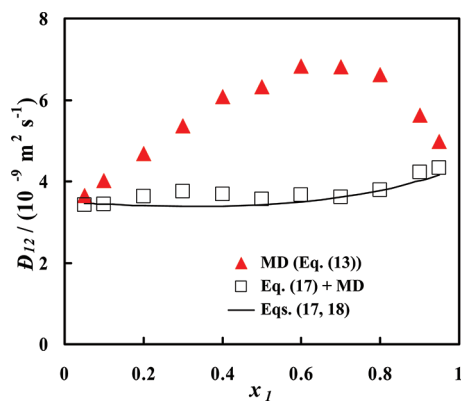


Figure 4. MS diffusivities in acetone (1)–methanol (2) mixtures at 298 K, 1 atm. Filled symbols are the computed MS diffusivities by this work using MD simulations (eq 13). Open symbols are the predictions using the Darken equation (eq 17) with the self-diffusivities taken from MD simulations. The solid line represents the predictions using the Darken equation (eq 17) with the self-diffusivities predicted using eq 18.

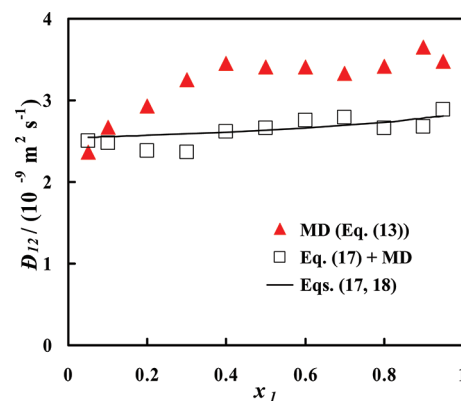


Figure 6. Fick diffusivities in acetone (1)–methanol (2) mixtures at 298 K, 1 atm. Filled symbols represent Fick diffusivities calculated using the computed Γ and MS diffusivities \bar{D}_{12} by this work. Open symbols are the predictions of Fick diffusivities using Γ obtained from experiments⁵⁰ and MS diffusivities predicted using the Darken equation (eq 17). Self-diffusivities appearing in Darken equation are estimated using eq 18. The solid line is the experimental data taken from ref 41.

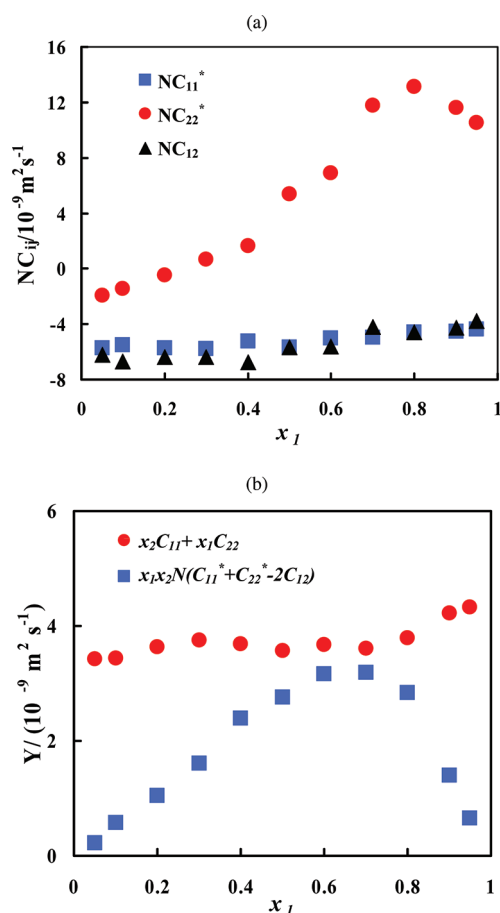


Figure 5. Velocity cross-correlations (see eqs 14 and 16) in acetone (1)–methanol (2) mixtures at 298 K, 1 atm.

strongly depend on the concentration, and this strong dependence is not captured by the Darken equation. It is important to consider the assumptions made in the derivation of the Darken

equation; i.e., velocity cross-correlations are much smaller than velocity autocorrelations. The deviations between MD simulations and predictions using the Darken equation suggest that this assumption does not hold in acetone–methanol mixtures. In Figure 5a, we plot the intensive terms NC_{ii}^* and NC_{ij} (see eqs 14 and 15) as a function of the concentration. We split the terms in eq 16 into a velocity autocorrelation part, i.e., $(x_2C_{11} + x_1C_{22})$, and a velocity cross-correlation part, i.e., $x_1x_2N(C_{11}^* + C_{22}^* - 2C_{12})$. The values of these two terms are plotted in Figure 5b. When the concentration of one of the components is small, the terms involving velocity cross-correlations are much smaller than those for velocity autocorrelations. The prediction using the binary Darken equation is reasonable in this regime. In more concentrated systems, the terms describing velocity cross-correlations are comparable to those for velocity autocorrelations resulting in the failure of the binary Darken equation. This is mainly due to the strong correlations between distinct molecules of methanol (see the line for NC_{11}^* in Figure 5a).

Figure 6 shows the Fick diffusivities in acetone–methanol mixtures obtained from the different approaches. Computed Fick diffusivities from MD simulations are in excellent agreement with experimental data. Combining the Darken equation with experimental values for the thermodynamic factor clearly results in significant deviations. Although both the thermodynamic factor and the MS diffusivity strongly depend on concentration, these effects are to a large degree canceled for the Fick diffusivity.

4.3. Diffusion in Acetone–Tetrachloromethane. Figure 7 compares the densities in acetone– CCl_4 mixtures at 1 atm. Reference 47 reported mixture densities at 298 K which are larger than the computed densities in this work. Kumar et al. also measured the densities of same mixtures at different temperatures.⁴⁸ Their results showed that the mixture densities are not very sensitive to the temperature. It is quite surprising to see such a big jump (ca. 10%) in density when temperature is raised from 298 to 303 K. It is unclear to us whether this effect is real or due to an error in the experiments.

Figure 8 shows the thermodynamic factor as a function of concentration. Again, excellent agreement between simulations and experiments is obtained. The nonideality is most pronounced

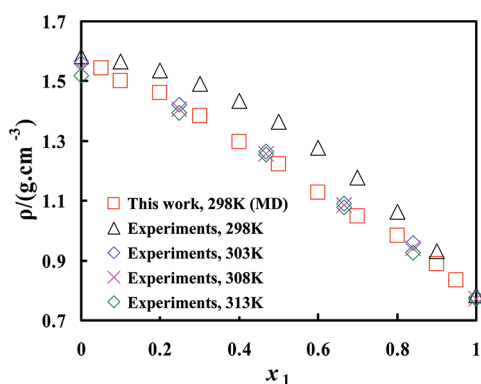


Figure 7. Densities of acetone (1)–CCl₄ (2) mixtures at 1 atm. Squares are the computed densities by this work using MD simulations at 298 K. Triangles are the experimental density taken from ref 47 at 298 K. Diamonds are the experimental density measured by Kumar et al.⁴⁸

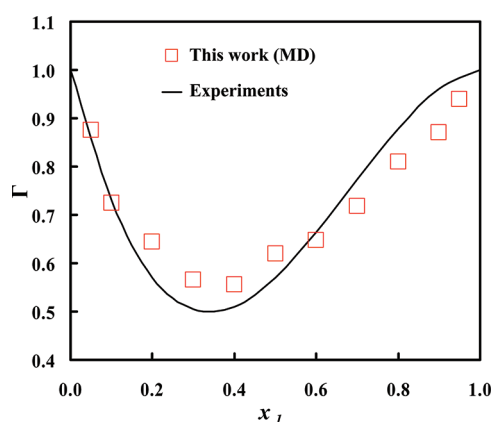


Figure 8. Thermodynamic factor Γ in acetone (1)–CCl₄ (2) mixtures at 298 K, 1 atm. Squares are the computed Γ by this work using MD simulations (error bars are equal to the symbol size). The solid line is Γ calculated from experimental VLE data taken from ref 50.

at a mole fraction of acetone of 0.35. This is observed both in experiments and simulations.

Figure 9 compares the self-diffusivities obtained from the different approaches. We observed that the computed self-diffusivities moderately increase with increasing concentration of acetone. In contrast, the experimental results show a stronger dependence of the self-diffusivities on concentration. The predictions using eq 18 agree well with the simulation results.

Figure 10 shows the computed and predicted MS diffusivities. The Darken equation suggests a linear relation between MS diffusivities and concentration while the computed MS diffusivities do not show this behavior. In Figure 11, we plot the values of the velocity cross-correlations and velocity autocorrelations as a function of the concentration (see eqs 14–16). Compared to the acetone–methanol system (Figure 5), the contributions of velocity cross-correlations in acetone–CCl₄ mixtures are smaller than those in acetone–methanol mixtures. This may suggest that the Darken equation works better in acetone–CCl₄ mixtures, see Figures 4 and 10. Figure 11a also shows that the terms C_{11}^* , C_{22}^* , and C_{12} are all of the same order of magnitude.

Using the thermodynamic factor Γ and MS diffusivities \mathfrak{D}_{ij} listed in Figures 8 and 10, we calculated Fick diffusivities as a

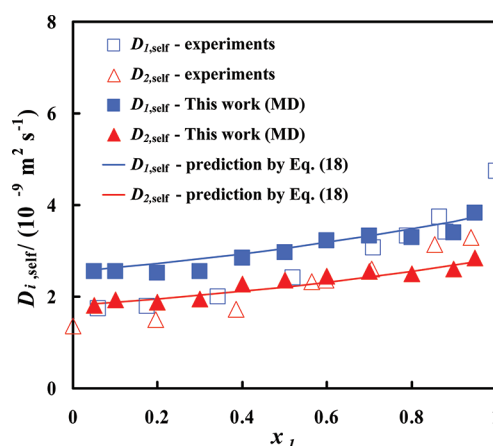


Figure 9. Self-diffusivities in acetone (1)–CCl₄ (2) mixtures at 298 K, 1 atm. Filled symbols are the computed diffusivities by this work using MD simulations. Open symbols are the experimental results taken from ref 41. Solid lines are the predictions using eq 18.

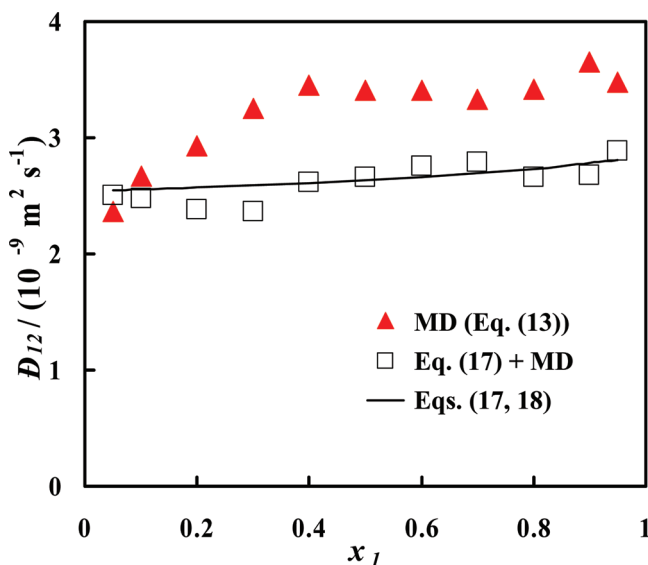


Figure 10. MS diffusivities in acetone (1)–CCl₄ (2) mixtures at 298 K, 1 atm. Filled symbols are the computed MS diffusivities by this work using MD simulations (eq 13). Open symbols are the predictions using the Darken equation with the self-diffusivities computed from MD simulations. The solid line represents the predictions using Darken equation (eq 17) with the self-diffusivities estimated by eq 18.

function of concentration, see Figure 12. Again, an excellent agreement between the computed Fick diffusivities from equilibrium MD simulations and the ones reported by experimental work is obtained. The comparison of Fick diffusivities in Figure 12 clearly shows that we can quantitatively predict Fick diffusivities in a consistent way from equilibrium MD simulation. As velocity cross-correlations are relatively small for this system, the predicted Fick diffusivities using the Darken equation and eqs 8 and 18 are in reasonable agreement with the experimental results. However, this agreement cannot be expected in general as the level of agreement strongly depends on the quality of the predictive model for MS diffusivities (here, the binary Darken equation).

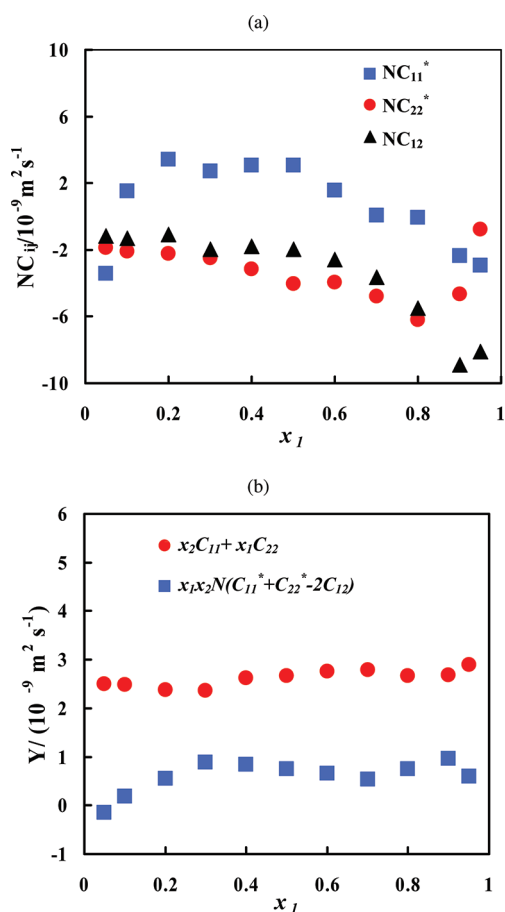


Figure 11. Velocity cross-correlations (see eqs 14 and 16) in acetone (1)–CCl₄ (2) mixtures at 298 K, 1 atm.

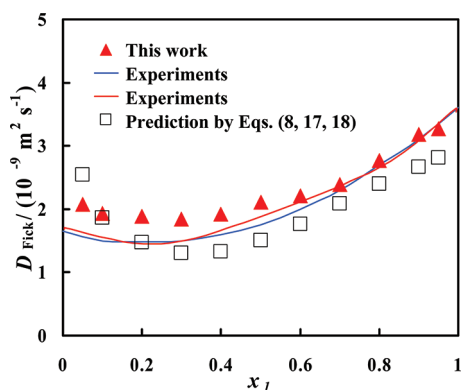


Figure 12. Fick diffusivities in acetone (1)–CCl₄ (2) mixtures at 298 K, 1 atm. Filled symbols represent Fick diffusivities calculated using the computed Γ and MS diffusivities \mathfrak{D}_{12} in this work. Open symbols are the predictions of Fick diffusivities using Γ obtained from experiments⁵⁰ and MS diffusivities predicted using the Darken equation (eq 17). Self-diffusivities appearing in the Darken equation are estimated using eq 18. Blue and red lines represent the experimental data taken from refs 51 and 52.

Indeed, predictive models may not work well (or even significantly fail) in systems in which molecules are highly associated.^{10,49}

5. CONCLUSION

We presented an efficient method to compute Fick diffusivities from equilibrium MD simulations without requiring any additional knowledge such as, e.g., the equation of state of the system. Therefore, the computed Fick diffusivities exclusively follow from the intermolecular interactions in the system, and no concentration gradients are present during the simulations. The key ingredient of this approach is the application of our novel method to extract the thermodynamic factor from equilibrium MD. The described approach was tested for two binary systems, acetone–methanol and acetone–CCl₄. Excellent agreement between molecular simulation and experimental results was found for Fick and MS diffusivities, as well as the thermodynamic factor. The binary Darken equation is not applicable to these systems as velocity cross-correlations have a large effect on the computed Onsager coefficients. Our approach is in principle directly applicable to obtain Fick diffusivities from simulations for multicomponent systems ($n \geq 3$).

AUTHOR INFORMATION

Corresponding Author

*E-mail: t.j.h.vlugt@tudelft.nl.

ACKNOWLEDGMENT

This work was performed as part of the Cluster of Excellence “Tailor-Made Fuels from Biomass”, which is funded by the Excellence Initiative by the German federal and state governments to promote science and research at German universities. S.K.S., S.K., and T.J.H.V. acknowledge financial support from NWO-CW through an ECHO grant. This work was also sponsored by the Stichting Nationale Computerfaciliteiten (National Computing Facilities Foundation, NCF) for the use of supercomputing facilities, with financial support from the Nederlandse Organisatie voor Wetenschappelijk onderzoek (Netherlands Organization for Scientific Research, NWO).

REFERENCES

- (1) Krishna, R.; Wesselingh, J. A. *Chem. Eng. Sci.* **1997**, *52*, 861–911.
- (2) Hendriks, E.; Kontogeorgis, G. M.; Dohrn, R.; de Hemptinne, J. C.; Economou, I. G.; Zilnik, L. F.; Vesovic, V. *Ind. Eng. Chem. Res.* **2010**, *49*, 11131–11141.
- (3) Bardow, A.; Kriesten, E.; Voda, M. A.; Casanova, F.; Blümich, B.; Marquardt, W. *Fluid Phase Equilib.* **2009**, *278*, 27–35.
- (4) Taylor, R.; Krishna, R. *Multicomponent Mass Transfer*; Wiley: New York, 1993.
- (5) Kjelstrup, S.; Bedeaux, D. *Non-Equilibrium Thermodynamics of Heterogeneous Systems*; World Scientific: Singapore, 2008.
- (6) Kuiken, G. D. C. *Thermodynamics of Irreversible Processes: Applications to Diffusion and Rheology*, 1st ed.; Wiley: New York, 1994.
- (7) Wambui Mutoru, J.; Firoozabadi, A. *J. Chem. Thermodyn.* **2011**, *43*, 1192–1203.
- (8) Krishna, R.; van Baten, J. M. *Ind. Eng. Chem. Res.* **2005**, *44*, 6939–6947.
- (9) Liu, X.; Vlugt, T. J. H.; Bardow, A. *Fluid Phase Equilib.* **2011**, *301*, 110–117.
- (10) Liu, X.; Bardow, A.; Vlugt, T. J. H. *Ind. Eng. Chem. Res.* **2011**, *50*, 4776–4782.
- (11) Liu, X.; Vlugt, T. J. H.; Bardow, A. *Ind. Eng. Chem. Res.* **2011**, *50*, 10350–10358.
- (12) Liu, X.; Vlugt, T. J. H.; Bardow, A. *J. Phys. Chem. B* **2011**, *115*, 8506–8517.

- (13) Fernandez, G. A.; Vrabec, J.; Hasse, H. *Int. J. Thermophys.* **2005**, *26*, 1389–1407.
- (14) van de Ven-Lucassen, I. M. J. J.; Vlugt, T. J. H.; van der Zanden, A. J. J.; Kerkhof, P. J. A. M. *Mol. Phys.* **1998**, *94*, 495–503.
- (15) Wheeler, D. R.; Newman, J. *J. Phys. Chem. B* **2004**, *108*, 18362–18367.
- (16) Wheeler, D. R.; Newman, J. *J. Phys. Chem. B* **2004**, *108*, 18353–18361.
- (17) Keffer, D. J.; Adhangale, A. *Chem. Eng. J.* **2004**, *100*, 51–69.
- (18) Keffer, D. J.; Edwards, B. J.; Adhangale, P. *J. Non-Newtonian Fluid Mech.* **2004**, *120*, 41–53.
- (19) Taylor, R.; Kooijman, H. A. *Chem. Eng. Commun.* **1991**, *102*, 87–106.
- (20) Medvedev, O. O.; Shapiro, A. A. *Fluid Phase Equilib.* **2004**, *225*, 13–22.
- (21) Maginn, E. J.; Bell, A. T.; Theodorou, D. N. *J. Phys. Chem.* **1993**, *97*, 4173–4181.
- (22) Tsige, M.; Grest, G. S. *J. Chem. Phys.* **2004**, *120*, 2989–2995.
- (23) Tsige, M.; Grest, G. S. *J. Chem. Phys.* **2004**, *121*, 7513–7519.
- (24) Keffer, D. J.; Gap, C. Y.; Edwards, B. J. *J. Phys. Chem. B* **2005**, *109*, 5279–5288.
- (25) Zabala, D.; Nieto-Draghi, C.; de Hemptinne, J. C.; López de Ramos, A. L. *J. Phys. Chem. B* **2008**, *112*, 16610–16618.
- (26) Schnell, S. K.; Liu, X.; Simon, J. M.; Bardow, A.; Bedeaux, D.; Vlugt, T. J. H.; Kjelstrup, S. *J. Phys. Chem. B* **2011**, *115*, 10911–10918.
- (27) Schnell, S. K.; Vlugt, T. J. H.; Simon, J. M.; Bedeaux, D.; Kjelstrup, S. *Chem. Phys. Lett.* **2011**, *504*, 199–201.
- (28) Frenkel, D.; Smit, B. *Understanding Molecular Simulation: from Algorithms to Applications*, 2nd ed.; Academic Press: San Diego, 2002.
- (29) Allen, M. P.; Tildesley, D. J. *Computer Simulation of Liquids*; Oxford University Press: New York, 1987.
- (30) Rapaport, D. *The Art of Molecular Dynamics Simulation*, 2nd ed.; Cambridge University Press: Cambridge, U.K., 2004.
- (31) Dubbeldam, D.; Ford, D. C.; Ellis, D. E.; Snurr, R. Q. *Mol. Simul.* **2009**, *35*, 1084–1097.
- (32) Darken, L. S. *Trans. Am. Inst. Min., Metall. Pet. Eng.* **1948**, *175*, 184–201.
- (33) Kirkwood, J. G.; Buff, F. P. *J. Chem. Phys.* **1951**, *19*, 774–777.
- (34) Ben-Naim, A. *Molecular Theory of Solutions*; Oxford University Press: Oxford, 2006.
- (35) Shi, W.; Maginn, E. J. *J. Chem. Theory Comput.* **2007**, *3*, 1451–1463.
- (36) Shi, W.; Maginn, E. J. *J. Comput. Chem.* **2008**, *29*, 2520–2530.
- (37) Ruckenstein, E.; Shulgin, I. *Fluid Phase Equilib.* **2001**, *180*, 345–359.
- (38) Perera, A.; Zoranic, L.; Sokolic, F.; Mazighi, R. *J. Mol. Liq.* **2011**, *159*, 52–59.
- (39) Jorgensen, W. L. *J. Phys. Chem.* **1986**, *90*, 1276–1284.
- (40) Tummala, N. R.; Striolo, A. *J. Phys. Chem. B* **2008**, *112*, 10675–10683.
- (41) Hardt, A. P.; Anderson, D. K.; Rathbun, R.; Mar, B. W.; Babb, A. L. *J. Phys. Chem.* **1959**, *63*, 2059–2061.
- (42) Toryanik, A. I.; Taranenko, V. N. *J. Struct. Chem.* **1988**, *28*, 714–719.
- (43) Kamei, Y. O.; Sumie, H. *J. Chem. Phys.* **1974**, *61*, 2227–2230.
- (44) Derlacki, Z. J.; Easteal, A. J.; Edge, A. V. J.; Woolf, L. A.; Roksandic, Z. *J. Phys. Chem.* **1985**, *89*, 5318–5322.
- (45) Campbell, A. N.; Kartzmark, E. M. *J. Chem. Thermodyn.* **1973**, *5*, 163–172.
- (46) Noda, K.; Ohashi, M.; Ishida, K. *J. Chem. Eng. Data* **1982**, *27*, 326–328.
- (47) Timmermans, J. *The Physico-Chemical Constants of Binary Systems in Concentrated Solutions*; Interscience Publishers: New York, 1959.
- (48) Kumar, R.; Jayakumar, S.; Kannappan, V. *Indian J. Pure Appl. Math.* **2008**, *46*, 169–175.
- (49) Tyrell, H. J. V.; Harris, K. R. *Diffusion in Liquids*; Butterworths: London, 1984.
- (50) Gmehling, J.; Onken, U. *Vapor-Liquid Equilibrium Data Collection*; DECHEMA: Frankfurt, Germany, 2005.
- (51) Alimadadian, A.; Colver, C. P. *Can. J. Chem. Eng.* **1976**, *54*, 208–213.
- (52) Anderson, D. K.; Hall, J. R.; Babb, A. L. *J. Phys. Chem.* **1958**, *62*, 404–408.